HHS Public Access

Author manuscript

J Med Chem. Author manuscript; available in PMC 2017 September 22.

Published in final edited form as:

J Med Chem. 2017 June 22; 60(12): 5222–5227. doi:10.1021/acs.jmedchem.7b00432.

A Facile Radiolabeling of [^{18}F]FDPA via Spirocyclic Iodonium Ylides: Preliminary PET Imaging Studies in Preclinical Models of Neuroinflammation

Lu Wang[†,§], **Ran Cheng**[†,¶,§], **Masayuki Fujinaga**[‡,§], **Jian Yang**[#], **Yiding Zhang**[‡], **Akiko Hatori**[‡], **Katsushi Kumata**[‡], **Jing Yang**[#], **Neil Vasdev**[†], **Yunfei Du**[¶], **Chongzhao Ran**[#], **Ming-Rong Zhang**[*,‡], and **Steven H. Liang**[*,†]

[†]Division of Nuclear Medicine and Molecular Imaging, Massachusetts General Hospital & Harvard Medical School, Boston, MA, USA

[‡]Department of Radiopharmaceutics Development, National Institute of Radiological Sciences, National Institutes for Quantum and Radiological Science and Technology, Chiba, Japan

[¶]School of Pharmaceutical Science and Technology, Tianjin University, Tianjin, China

[#]Athinoula A. Martinos Center for Biomedical Imaging, Massachusetts General Hospital & Harvard Medical School, Boston, MA, USA

Abstract

A suitable TSPO PET ligand may visualize and quantify neuroinflammation in living brain. Herein we report a ^{18}F-ligand, **[^{18}F]2** ([^{18}F]FDPA) is radiolabeled in high yield and high specific activity based on our spirocyclic iodonium ylide (SCIDY) strategy. **[^{18}F]2** demonstrated saturable specific binding to TSPO, substantially-elevated brain uptake and slow washout of bound PET signal in the preclinical models of brain neuroinflammation (cerebral ischemia and Alzheimer's disease).

TOC image

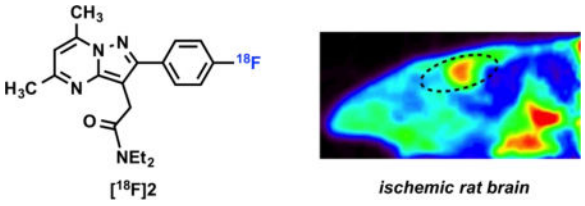

[*]**Corresponding Author**: Tel: +81 43 382 3709. Fax: +81 43 206 3261. zhang.ming-rong@qst.go.jp.; Tel: +1 617 726 6106. Fax: +1 617 726 6107. liang.steven@mgh.harvard.edu.

[§]Author Contributions

L.W., R. C. and M. F. contributed equally to this work.

Supporting Information

Synthetic and analytical results for all compounds; animal models and imaging methods; supplemental figures. This material is available free of charge via the Internet at http://pubs.acs.org.

INTRODUCTION

The translocator protein 18 kDa (TSPO) is a five trans-membrane domain protein and located with outer mitochondrial membrane. TSPO is expressed predominantly in steroid-synthesizing endocrine organs including heart, kidneys, adrenal cortex, testis or ovary.[1] One of the most well-characterized functions of TSPO is its involvement in the translocation of cholesterol from the outer to the inner mitochondrial membrane,[2] which is critical to the synthesis of steroids. In the central nervous system (CNS), TSPO is dramatically upregulated in neuroinflammatory conditions (activated microglial cells).[3, 4] Abnormal overexpression of TSPO has been found as a pivotal pathological signal in the progression of many other neurological disorders. In particular, neuroinflammation occurs at the pre-plaque stage[5] of Alzheimer's disease (AD) and serves as a major driving force.[6] Recent studies have also revealed that the TSPO expression was closely associated with infarction induced by ischemia.[7] Therefore, TSPO is a potential biomarker for detecting inflammation associated with brain disorders, and for monitoring treatment response of anti-inflammatory therapies.

Positron emission tomography (PET) is a non-invasive imaging technology that is capable of visualizing and quantifying biochemical and pharmacological processes *in vivo*. A TSPO-specific PET ligand is utilized as a translational imaging tool to evaluate the status of neuroinflammation (activated microglia) in living brain.[8, 9] [^{11}C]PK11195 was the first extensively evaluated PET ligand for TSPO; however, low signal-to-noise ratio and high non-specific binding hampered its further advance.[10] Intensive efforts therefore have been made to improve PET imaging quality and quantitative process with the development of a rich library of TSPO PET ligands.[11–13] Particularly a PET ligand **[^{18}F]1** ([^{18}F]DPA-714; Figure 1), developed by James and Kassiou *et al*, has shown improved bioavailability, lower nonspecific binding, and higher non-displaceable binding potential (BP_{ND}).[14, 15] Initial evaluation of this radiopharmaceutical in healthy human volunteers validated its biodistribution profile towards TSPO.[16] Clinical PET studies using **[^{18}F]1** were further conducted on patients with amyotrophic lateral sclerosis,[17] post-stroke[18] and AD,[19] demonstrating this ligand may be useful in assessing the extent of neuroinflammation.

N,N-diethyl-2-(2-(4-[^{18}F]fluorophenyl)-5,7-dimethylpyrazolo[1,5-a]pyrimidine-3-yl)-acetamide **[^{18}F]2** ([^{18}F]FDPA), a fluoroaryl analog of **[^{18}F]1**, in which the fluorine atom is directly attached to terminal aromatic ring, is another promising PET ligand (Figure 1). Its intrinsic structure (aryl-^{18}F bond) offers an improved metabolic profile via substantially-reduced formation of radiolabeled metabolites in brain and plasma compared with **[^{18}F]1** as observed by Solin and Dollé *et al*.[20, 21] Several radiofluorination reactions were reported to prepare **[^{18}F]2** via [^{18}F]fluoride ion under various labeling conditions, including nitroarene, aryltrimethylammonium salt and diaryliodomium salt as precursors, that resulted in limited radiochemical conversions (< 3%).[22] Electrophilic fluorination starting with carrier-added [^{18}F]F_2 to prepare [^{18}F]Selectfluor as a labeling reagent was recently performed by Solin and co-workers, to prepare **[^{18}F]2**, and resulted in 15 ± 3% decay corrected yields with a low specific activity of 7.8 ± 0.5 GBq/μmol (0.21 ± 0.01 Ci/μmol).[23] However, because a low-cold-mass PET ligand injection is critical to detect inflammatory events,[24, 25] there is an

unmet and urgent need for **[^{18}F]2** with high specific activity to evaluate the potential of this radioligand in PET imaging of neuroinflammation.

On the basis of our previous work, precise radiofluorination of non-activated aromatics can be achieved with spirocyclic iodonium ylide (SCIDY) precursors.[26–29] These bench-stable precursors provide efficient, regiospecific and direct radiolabeling via [^{18}F]fluoride, demonstrating a broad substrate scope for non-activated and/or sterically-hindered (hetero)arenes. The operation is simple, metal-free and suitable for routine and automated production. Herein, we report an efficient radiosynthesis of **[^{18}F]2** based on SCIDY precursors from no-carrier added [^{18}F]fluoride and preliminary PET imaging evaluation in preclinical models of ischemia and AD.

RESULTS AND DISCUSSION

Chemistry

As shown in Scheme 1, we developed an efficient route and improved the literature procedure[30] to obtain non-radioactive standard **10** (FDPA), and the key intermediate **11** for our SCIDY strategy. Microwave-assisted synthesis was utilized to assemble *N,N*-diethylamide **6** with dramatically-reduced reaction time (40 min) while maintaining a good yield (55%). The cyclization reaction triggered by hydrazine and acetic acid, led to fluoroaminopyrazole **8** in 88% yield. Finally, condensation between **8** and acetylacetone afforded **10** as a white crystalline solid in 75% yield. The key compound **11** was also prepared in an analogous synthetic route with an overall yield of 41% in three steps from 3-(4-iodophenyl)-3-oxopropanenitrile **4**. We found that oxidation of **11** by using Oxone in mixed solvents of $CHCl_3$ and trifluoroacetic acid was critical for this type of transformation, leading to the corresponding iodo(III) intermediate **12** in *ca.* 60% conversion. The intermediate was used without further purification in the subsequent coupling reactions with spirocyclic auxiliaries (SPI5 and SPIAd)[29] to afford SCIDY precursors **13** (22%, two steps from **11**) and **14** (34%, two steps from **11**), respectively.

Pharmacology

In vitro binding affinity of **10** for TSPO was measured from competitive binding of TSPO-selective radioligand [^{3}H]PK11195 (Figure S1). **10** showed excellent binding affinity (K_i: 2.0 ± 0.8 nM) which is consistent with prior reports[31] and comparable with that of DPA-714 (K_i: 7.0 ± 0.4 nM).[14] The selectivity of **10** towards central benzodiazepine receptor (CBR) binding was reported as K_i > 1 mM,[22] in comparison to that of DPA-714 (K_i > 10 μM).[14] These results indicated that **[^{18}F]2** could be utilized to study *in vivo* binding profiles for TSPO by PET.

Radiochemistry

Based on our prior reports of utilizing SCIDY precursors to enable radiofluorination on non-activated arenes from no-carrier added [^{18}F]fluoride,[26, 29] we developed an efficient radiolabeling method from SCIDY precursor **14** to produce **[^{18}F]2**. Specifically, we carried out comprehensive optimization of radiofluorination conditions, including bases, solvents, reaction temperatures and precursor loadings (Figure 2). We first set out the

radiofluorination with **14** using different types and loading amounts of bases, including tetraethylammonium bicarbonate (TEAB) and K_2CO_3/K_{222} in DMF. Unfortunately, under these conditions only trace amounts of **[^{18}F]2** were detected. These fruitless results promoted us to study the thermostability of SCIDY precursors. While compound **14** alone showed no decomposition when heating at 120 °C for 10 min, the addition of TEAB (1 mg) led to a rapid decomposition even without heating, which indicates alternative milder bases/additives may be necessary to achieve high radiolabeling efficiency (Figure S2). To our delight, combination of $K_2C_2O_4/K_{222}$ gave the desired product **[^{18}F]2** with >20% radiochemical conversion (RCC). Furthermore two quaternary alkylammonium salts, namely, tetrabutylammonium methanesulfonate (TBAOMs)[32] and tetraethylammonium perchlorate ($TEAOCl_4$) were identified as the most promising additives (> 30% RCCs) for further evaluation (Figure 2A & Figure S3). By optimizing reaction time and temperature we found that TBAOMs was superior to $TEAOCl_4$, and RCCs reached to 40 ± 3% (n = 3) at 120 °C for 15 min (Figure 2B & 2C). Together with solvent effect (Figure 2D) and the amounts of precursor loading (Figure S4), we identified that the combination of 12 mg of TBAOMs, 1 mg of SCIDY precursor **14** in CH_3CN at 120 °C for 15 min provided the highest RCC of 63 ± 5% (n = 6). In addition, we also tested SPI5-based SCIDY precursor **13** under the optimal conditions (Figure S5), which only provided 16 ± 3% RCC (n = 3). These results were consistent with our prior observation that SPIAd precursors were more efficient than SPI5 precursors under ^{18}F-labeling reactions.[29] As a result, the radiosynthesis of **[^{18}F]2** was achieved in 45 ± 8% decay-corrected yield within 80 min with >99% radiochemical and chemical purity and specific activity of 96 ± 22 GBq/μmol (2.6 ± 0.6 Ci/μmol; see experimental section). The identity of **[^{18}F]2** was confirmed by co-injection with **10** (Figure S6). No radiolysis was observed up to 120 min after formulation. **[^{18}F]2** was stable *in vitro* in mouse serum at 37 °C for 120 min. The efficient radiosynthesis with high specific activity, radiochemical purity and stability enabled the subsequent *ex vivo* biodistribution and preclinical *in vivo* PET imaging studies.

Lipophilicity

Lipophilicity can be used, in part, as a predictive value for assessing blood brain barrier (BBB) permeability with an optimal range of 1.0–3.5.[33] Using liquid-liquid partition ("the shake flask method"), Log$D_{7.4}$ value of **[^{18}F]2** was determined to be 2.34 ± 0.05 (n = 5), which is comparable with several reported TSPO radioligands such as [^{18}F]DPA-714 (**[^{18}F]1**; Log$D_{7.4}$ 2.44)[14] and [^{18}F]GE-180 (Log$D_{7.4}$ 2.95).[31]

Whole body biodistribution studies

The uptake, distribution and clearance of **[^{18}F]2** were studied in mice at three time points (2, 25 and 45 min) post injection (Figure 3, Table S1 and S2). At 2 min p.i., high uptake (>5 %ID/g) was observed in the lungs, heart, liver, kidneys, pancreas and adrenal glands. After the initial phase the radioactivity levels in most tissues decreased rapidly, while the signals in the kidney, spleen and adrenal glands continued to increase during the whole period. The radioligand was efficiently cleared from blood (2 min/45 min ratio >10), and high uptake of **[^{18}F]2** in the liver, kidney and small intestine indicated urinary and hepatobiliary excretion, as well as possible intestinal re-uptake. The uptake of **[^{18}F]2** in the

present study is consistent with the distribution of TSPO in mice, as high expression in the lungs, heart, kidneys and adrenal glands has been previously observed.[1] In particular, since TSPO expression in microglia cells of normal brain has been found to be in a low level,[34] brain uptake of **[^{18}F]2** was moderate with 3.69 %ID/g at 2 min p.i., and the radioactivity washout was reasonable with 1.15 %ID/g at 45 min time point (2 min/45 min ratio 3.2). In addition, negligible bone uptake was detected (<1 %ID/g), showing little or no defluorination occurred *in vivo*, which was also confirmed by PET imaging studies (Figure S7). Based on these results, we further evaluated if **[^{18}F]2** is a suitable PET ligand targeting TSPO in preclinical models of neuroinflammatory brain.

PET imaging studies in preclinical models of neuroinflammatory brain

Due to the low TSPO expression in normal brain,[34] we utilized a focal cerebral ischemic rat model (see section 10 in SI) in which TSPO expression was up-regulated with activated microglia[35] while the blood-brain barrier was intact or not seriously disrupted.[36] As shown in Figure 4, PET images and time-activity curves of **[^{18}F]2** showed maximum uptake in the ipsilateral side (ischemic site) reached a peak of 1.20 SUV at 10 min. Blockade with PK11195 (3 mg/kg) decreased PET signal by *ca.* 80%, indicating high *in vivo* specificity and low non-specific binding. The $SUV_{(2/40min)}$ ratio of 2.9 showed a rapid washout rate of non-specific binding under blocking conditions. In the contralateral side, **[^{18}F]2** showed limited peak brain uptake (0.54 SUV) and marginal changes between baseline and blocking conditions. We also observed a rapid clearance of non-specific binding ($SUV_{2/40min}$ = 5.9) probably attributed to low expression of TSPO in normal brain.[34] High ipsilateral to contralateral ratios at 10 min and 90 min p.i. were determined as 5.41 ± 0.12 and 4.26 ± 0.34, respectively. Pretreatment with PK11195 also substantially diminished heterogeneous radioactive signals between ipsilateral and contralateral sides.

We also carried out a simplified reference-tissue model (SRTM) analysis and determined BP_{ND} using the contralateral side as the reference region.[36] The BP_{ND} values in the ipsilateral sides were determined to be 4.02 ± 1.32 ($p < 0.05$) for **[^{18}F]2**, which was higher than [^{11}C]PK11195 (1.59 ± 0.33, $p < 0.05$).[36]

Liu *et al.* demonstrated that TSPO was mainly expressed in activated microglia in APP/PS1 transgenic mouse brains by immunofluorescence studies between TSPO and Aβ as well as the association of Aβ deposition and TSPO-positive microglia in human AD brain sections.[37] Thus as proof of concept, we explored *in vivo* binding profile of **[^{18}F]2** in a transgenic mouse model (APP/PS1) of AD. **[^{18}F]2** rapidly crossed the BBB and increased to 1.50 ± 0.13 SUV at 3 min p.i., demonstrating 1.6-fold higher peak brain uptake and slow washout (possibly attributed to increased specific and non-specific binding) in APP/PS1 brain compared with age-matched control (Figure 5).

In vitro autoradiography

The binding specificity of **[^{18}F]2** to TSPO was further confirmed by autoradiography studies in ischemia and AD brains. The ipsilateral side of ischemic rat brain showed substantially increased signal levels than that of contralateral side (ratio 7:1; Figure 6). The difference in radioactivity levels between the ipsilateral and contralateral sides was diminished by co-

incubation with PK11195 (Figure 6B), leaing to a dramatic reduction (>98%) of ipsilateral binding (Figure 6C). We also noted increased whole brain uptake in APP/PS1 mouse brain slices compared with age-matched controls (Figure S8). These *in vitro* findings are consistent with the *in vivo* binding specificity of **[^{18}F]2** by PET studies.

CONCLUSION

The SCIDY-based methodology provides a high-yield and high-specific-activity radiosynthesis of **[^{18}F]2** that enabled preliminary PET studies in preclinical models of focal cerebral ischemia and Alzheimer's disease. These proof-of-concept results not only warrant **[^{18}F]2** as a promising imaging biomarker to elucidate the involvement of microglia activity in preclinical models of ischemia and AD, but also provide the basis for designing new pyrazolo[1,5-a]pyrimidine based TSPO PET ligands. Further validation including immunofluorescent staining, radiometabolite analysis, PET imaging studies in higher species among different polymorphism are outlined to evaluate the suitability of **[^{18}F]2** as a potential imaging tool for clinical translation.

EXPERIMENTAL SECTION

Preparation of SPIAd precursor 14

To a solution of **11** (50 mg, 0.11 mmol) in trifluoroacetic acid (0.39 mL) and chloroform (0.13 mL) was added Oxone (100mg, 0.165 mmol) under stirring. The mixture was stirred at room temperature for 60 min, then concentrated *in vacuo*. To the crude was added EtOH (0.8 mL), then a solution of SPIAd (25.3 mg, 0.11 mmol) in 10% Na_2CO_3 (0.5 mL), followed by additional 10% Na_2CO_3 (0.3 mL) to adjust to pH 9. The mixture was stirred at room temperature for 70 min, then diluted with H_2O (5 mL), extracted with CH_2Cl_2 (5 mL × 3). The combined organic layers were dried over $MgSO_4$ and concentrated *in vacuo*. The residue was purified by column chromatography on silica gel (0–10% MeOH in EtOAc) to afford ylide precursor **14** as a white solid (26.1 mg, 34% yield).

Radiolabeling of [^{18}F]2

[^{18}F]Fluoride solution (0.74–1.48 GBq; 20–40 mCi) was delivered and trapped on a Waters Sep-Pak light QMA cartridge (pretreated with 1 mL of 8.3% aqueous $NaHCO_3$ and 20 mL H_2O) by nitrogen gas. A solution of TBAOMs (12.0 mg) in CH_3CN/H_2O (v/v, 1/1, 1.0 mL) was used to elute [^{18}F]fluoride into a V-shaped vial sealed with a Teflon-lined septum. The vial was heated to 110 °C while nitrogen gas was passed through a P_2O_5-Drierite™ column into the vented vial. When no liquid was visible, it was removed from heat, anhydrous CH_3CN (1 mL) was added, then the heating was resumed until dryness. This step was repeated three times. The vial was then cooled to room temperature under nitrogen flow. A solution of precursor **14** (1.0 mg) in anhydrous CH_3CN (1 mL) was added into the reaction vial and heated at 120 °C for 12 min. CH_3CN/H_2O (v/v, 1/1, 2.0 mL) was added to the mixture, which was then injected to a semi-preparative HPLC system. HPLC purification was completed on a semi-preparative Phenomenex Luna C18 column (250 × 10 mm, 5 μm) eluting with CH_3CN/0.1 M NH_4•HCO_2(aq) (v/v, 1/1) at a flowrate of 5 mL/min. The retention time for **[^{18}F]2** was 17.5 min. The radioactive fraction corresponding to the desired

product was collected and diluted with 23 mL H_2O. The mixture was then loaded onto a C18 SPE cartridge (pre-activated with 5 mL EtOH followed by 10 mL of H_2O). The cartridge was washed with 20 mL of H_2O and dried by nitrogen gas for 5 min. The product **[^{18}F]2** was then eluted with 1.5 mL of CH_3OH, and collected in a sterile flask, evaporated to dryness by nitrogen gas at 60 °C for 20 min, and reformulated in a saline solution (3 mL) containing 100 μL of 25% ascorbic acid in H_2O and 100 μL of 20% Tween® 80 in ethanol. The synthesis time was *ca.* 80 min from end-of-bombardment. Radiochemical and chemical purity were measured by analytical HPLC (Phenomenex Luna C18, 250 × 4.6 mm, 5 μm, UV at 254 nm; CH_3CN/0.1 M NH_4•HCO_2(aq) (v/v, 7/3) at a flowrate of 1.0 mL/min). The identity of **[^{18}F]2** was confirmed by the co-injection with unlabeled **10**. Radiochemical yield was 45 ± 8% (decay-corrected) with >99% radiochemical purity and 96 ± 22 GBq/μmol (2.6 ± 0.6 Ci/μmol) specific activity.

Supplementary Material

Refer to Web version on PubMed Central for supplementary material.

Acknowledgments

We thank the National Institute of Mental Health's Psychoactive Drug Screening Program for the compound screening. R.C. is supported by China Scholarship Council (201506250036). S.H.L. is a recipient of an NIH career development award (DA038000).

ABBREVIATIONS

PET	positron emission tomography
TSPO	translocator protein
FDPA	*N,N*-diethyl-2-(2-(4-fluorophenyl)-5,7-dimethylpyrazolo[1,5-*a*]pyrimidin-3-yl)acetamide
SUV	standardized uptake value, BP_{ND}, non-displaceable binding potential
SRTM	simplified reference-tissue model
TAC	time-activity curve
%ID/g	percentage of injected dose per gram of wet tissue

References

1. Rupprecht R, Papadopoulos V, Rammes G, Baghai TC, Fan J, Akula N, Groyer G, Adams D, Schumacher M. Translocator protein (18 kDa) (TSPO) as a therapeutic target for neurological and psychiatric disorders. Nat Rev Drug Discovery. 2010; 9:971–988. [PubMed: 21119734]
2. Papadopoulos V, Baraldi M, Guilarte TR, Knudsen TB, Lacapere JJ, Lindemann P, Norenberg MD, Nutt D, Weizman A, Zhang MR, Gavish M. Translocator protein (18kDa): new nomenclature for the peripheral-type benzodiazepine receptor based on its structure and molecular function. Trends Pharmacol Sci. 2006; 27:402–409. [PubMed: 16822554]
3. Banati RB. Visualising microglial activation in vivo. Glia. 2002; 40:206–217. [PubMed: 12379908]
4. Galiegue S, Tinel N, Casellas P. The peripheral benzodiazepine receptor: a promising therapeutic drug target. Curr Med Chem. 2003; 10:1563–1572. [PubMed: 12871127]

5. Ferretti MT, Cuello AC. Does a pro-inflammatory process precede Alzheimer's disease and mild cognitive impairment? Curr Alzheimer Res. 2011; 8:164–174. [PubMed: 21345170]
6. Heneka MT, Carson MJ, El Khoury J, Landreth GE, Brosseron F, Feinstein DL, Jacobs AH, Wyss-Coray T, Vitorica J, Ransohoff RM, Herrup K, Frautschy SA, Finsen B, Brown GC, Verkhratsky A, Yamanaka K, Koistinaho J, Latz E, Halle A, Petzold GC, Town T, Morgan D, Shinohara ML, Perry VH, Holmes C, Bazan NG, Brooks DJ, Hunot S, Joseph B, Deigendesch N, Garaschuk O, Boddeke E, Dinarello CA, Breitner JC, Cole GM, Golenbock DT, Kummer MP. Neuroinflammation in Alzheimer's disease. Lancet Neurol. 2015; 14:388–405. [PubMed: 25792098]
7. Gerhard A, Schwarz J, Myers R, Wise R, Banati RB. Evolution of microglial activation in patients after ischemic stroke: a [^{11}C](R)-PK11195 PET study. Neuroimage. 2005; 24:591–595. [PubMed: 15627603]
8. Signore A, Mather SJ, Piaggio G, Malviya G, Dierckx RA. Molecular imaging of inflammation/infection: nuclear medicine and optical imaging agents and methods. Chem Rev. 2010; 110:3112–3145. [PubMed: 20415479]
9. Damont A, Roeda D, Dolle F. The potential of carbon-11 and fluorine-18 chemistry: illustration through the development of positron emission tomography radioligands targeting the translocator protein 18 kDa. J Labelled Comp Radiopharm. 2013; 56:96–104. [PubMed: 24285315]
10. Chauveau F, Boutin H, Van Camp N, Dolle F, Tavitian B. Nuclear imaging of neuroinflammation: a comprehensive review of [^{11}C]PK11195 challengers. Eur J Nucl Med Mol Imaging. 2008; 35:2304–2319. [PubMed: 18828015]
11. Ory D, Celen S, Verbruggen A, Bormans G. PET radioligands for in vivo visualization of neuroinflammation. Curr Pharm Des. 2014; 20:5897–5913. [PubMed: 24939192]
12. Turkheimer FE, Rizzo G, Bloomfield PS, Howes O, Zanotti-Fregonara P, Bertoldo A, Veronese M. The methodology of TSPO imaging with positron emission tomography. Biochem Soc Trans. 2015; 43:586–592. [PubMed: 26551697]
13. Albrecht DS, Granziera C, Hooker JM, Loggia ML. In vivo imaging of human neuroinflammation. ACS Chem Neurosci. 2016; 7:470–483. [PubMed: 26985861]
14. James ML, Fulton RR, Vercoullie J, Henderson DJ, Garreau L, Chalon S, Dolle F, Costa B, Guilloteau D, Kassiou M. DPA-714, a new translocator protein-specific ligand: synthesis, radiofluorination, and pharmacologic characterization. J Nucl Med. 2008; 49:814–822. [PubMed: 18413395]
15. Chauveau F, Van Camp N, Dolle F, Kuhnast B, Hinnen F, Damont A, Boutin H, James M, Kassiou M, Tavitian B. Comparative evaluation of the translocator protein radioligands ^{11}C-DPA-713, ^{18}F-DPA-714, and ^{11}C-PK11195 in a rat model of acute neuroinflammation. J Nucl Med. 2009; 50:468–476. [PubMed: 19223401]
16. Arlicot N, Vercouillie J, Ribeiro MJ, Tauber C, Venel Y, Baulieu JL, Maia S, Corcia P, Stabin MG, Reynolds A, Kassiou M, Guilloteau D. Initial evaluation in healthy humans of [^{18}F]DPA-714, a potential PET biomarker for neuroinflammation. Nucl Med Biol. 2012; 39:570–578. [PubMed: 22172392]
17. Corcia P, Tauber C, Vercoullie J, Arlicot N, Prunier C, Praline J, Nicolas G, Venel Y, Hommet C, Baulieu JL, Cottier JP, Roussel C, Kassiou M, Guilloteau D, Ribeiro MJ. Molecular imaging of microglial activation in amyotrophic lateral sclerosis. PLoS One. 2012; 7:e52941. [PubMed: 23300829]
18. Ribeiro MJ, Vercouillie J, Debiais S, Cottier JP, Bonnaud I, Camus V, Banister S, Kassiou M, Arlicot N, Guilloteau D. Could ^{18}F-DPA-714 PET imaging be interesting to use in the early post-stroke period? EJNMMI Res. 2014; 4:28. [PubMed: 25006546]
19. Golla SS, Boellaard R, Oikonen V, Hoffmann A, van Berckel BN, Windhorst AD, Virta J, Haaparanta-Solin M, Luoto P, Savisto N, Solin O, Valencia R, Thiele A, Eriksson J, Schuit RC, Lammertsma AA, Rinne JO. Quantification of [^{18}F]DPA-714 binding in the human brain: initial studies in healthy controls and Alzheimer's disease patients. J Cereb Blood Flow Metab. 2015; 35:766–772. [PubMed: 25649991]
20. Peyronneau MA, Saba W, Goutal S, Damont A, Dolle F, Kassiou M, Bottlaender M, Valette H. Metabolism and quantification of [^{18}F]DPA-714, a new TSPO positron emission tomography radioligand. Drug Metab Dispos. 2013; 41:122–131. [PubMed: 23065531]

21. Haaparanta-Solin M, Lopez-Picon F, Almajidi R, Takkinen J, Keller T, Krzyczmonik A, Forsback S, Kirjavainen A, Cacheux F, Damont A, Rinne JO, Dollé F, Solin O. PET imaging and ex vivo brain autoradiography in a mouse model of Alzheimers disease using the TSPO tracers [^{18}F]DPA-714 and [^{18}F]F-DPA. J Labelled Comp Radiopharm. 2015; 58:S272.
22. Damont A, Caillé F, Navarrete VM, Cacheux F, Kuhnast B, Dollé F. The pyrazolo[1,5-a]pyrimidine F-DPA: synthesis, in vitro characterization and radiolabeling with fluorine-18 using a nucleophilic approach. J Labelled Comp Radiopharm. 2015; 58:S180.
23. Keller, T., Krzyczmonik, A., Forsback, S., Picon, FR., Kirjavainen, AK., Takkinen, J., Rajander, J., Cacheux, F., Damont, A., Dolle, F., Rinne, JO., Haaparanta-Solin, M., Solin, O. Radiosynthesis and Preclinical Evaluation of [^{18}F]F-DPA, A novel pyrazolo[1,5a]pyrimidine acetamide TSPO radioligand, in healthy sprague dawley rats. Mol Imaging Biol. 2017. Published Online: January 12, 2017. https://link.springer.com/article/10.1007%2Fs11307-016-1040-z
24. Yui J, Hatori A, Kawamura K, Yanamoto K, Yamasaki T, Ogawa M, Yoshida Y, Kumata K, Fujinaga M, Nengaki N, Fukumura T, Suzuki K, Zhang MR. Visualization of early infarction in rat brain after ischemia using a translocator protein (18 kDa) PET ligand [^{11}C]DAC with ultra-high specific activity. Neuroimage. 2011; 54:123–130. [PubMed: 20705143]
25. Yui J, Hatori A, Yanamoto K, Takei M, Nengaki N, Kumata K, Kawamura K, Yamasaki T, Suzuki K, Zhang MR. Imaging of the translocator protein (18 kDa) in rat brain after ischemia using [^{11}C]DAC with ultra-high specific activity. Synapse. 2010; 64:488–493. [PubMed: 20175226]
26. Rotstein BH, Stephenson NA, Vasdev N, Liang SH. Spirocyclic hypervalent iodine(III)-mediated radiofluorination of non-activated and hindered aromatics. Nat Commun. 2014; 5:4365. [PubMed: 25007318]
27. Stephenson NA, Holland JP, Kassenbrock A, Yokell DL, Livni E, Liang SH, Vasdev N. Iodonium ylide-mediated radiofluorination of 18F-FPEB and validation for human use. J Nucl Med. 2015; 56:489–492. [PubMed: 25655630]
28. Wang L, Jacobson O, Avdic D, Rotstein BH, Weiss ID, Collier L, Chen X, Vasdev N, Liang SH. *Ortho*-stabilized ^{18}F-azido click agents and their application in PET imaging with single-stranded DNA aptamers. Angew Chem; Int Ed. 2015; 54:12777–12781.
29. Rotstein BH, Wang L, Liu RY, Patteson J, Kwan EE, Vasdev N, Liang SH. Mechanistic studies and radiofluorination of structurally diverse pharmaceuticals with spirocyclic iodonium(III) ylides. Chem Sci. 2016; 7:4407–4417. [PubMed: 27540460]
30. Tang D, McKinley ET, Hight MR, Uddin MI, Harp JM, Fu A, Nickels ML, Buck JR, Manning HC. Synthesis and structure-activity relationships of 5,6,7-substituted pyrazolopyrimidines: discovery of a novel TSPO PET ligand for cancer imaging. J Med Chem. 2013; 56:3429–3433. [PubMed: 23521048]
31. Wadsworth H, Jones PA, Chau WF, Durrant C, Fouladi N, Passmore J, O'Shea D, Wynn D, Morisson-Iveson V, Ewan A, Thaning M, Mantzilas D, Gausemel I, Khan I, Black A, Avory M, Trigg W. [^{18}F]GE-180: a novel fluorine-18 labelled PET tracer for imaging Translocator protein 18 kDa (TSPO). Bioorg Med Chem Lett. 2012; 22:1308–1313. [PubMed: 22244939]
32. Shi H, Braun A, Wang L, Liang SH, Vasdev N, Ritter T. Synthesis of ^{18}F-difluoromethylarenes from aryl (pseudo) halides. Angew Chem; Int Ed. 2016; 55:10786–10790.
33. Patel S, Gibson R. In vivo site-directed radiotracers: a mini-review. Nucl Med Biol. 2008; 35:805–815. [PubMed: 19026942]
34. Gavish M, Bachman I, Shoukrun R, Katz Y, Veenman L, Weisinger G, Weizman A. Enigma of the peripheral benzodiazepine receptor. Pharmacol Rev. 1999; 51:629–650. [PubMed: 10581326]
35. Thiel A, Heiss W-D. Imaging of microglia activation in stroke. Stroke. 2011; 42:507–512. [PubMed: 21164114]
36. Tiwari AK, Yui J, Fujinaga M, Kumata K, Shimoda Y, Yamasaki T, Xie L, Hatori A, Maeda J, Nengaki N, Zhang MR. Characterization of a novel acetamidobenzoxazolone-based PET ligand for translocator protein (18 kDa) imaging of neuroinflammation in the brain. J Neurochem. 2014; 129:712–720. [PubMed: 24484439]
37. Liu B, Le KX, Park MA, Wang S, Belanger AP, Dubey S, Frost JL, Holton P, Reiser V, Jones PA, Trigg W, Di Carli MF, Lemere CA. In vivo detection of age- and disease-related increases in

neuroinflammation by ^{18}F-GE180 TSPO microPET imaging in wild-type and Alzheimer's transgenic mice. J Neurosci. 2015; 35:15716–15730. [PubMed: 26609163]

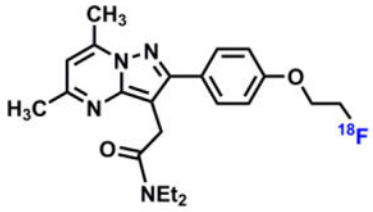

[^{18}F]1 ([^{18}F]DPA-714)

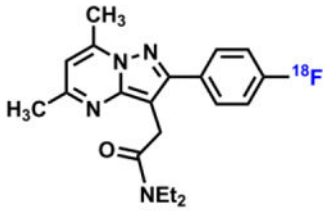

[^{18}F]2 ([^{18}F]FDPA)

Figure 1.
Chemical structures of **[^{18}F]1** and **[^{18}F]2**

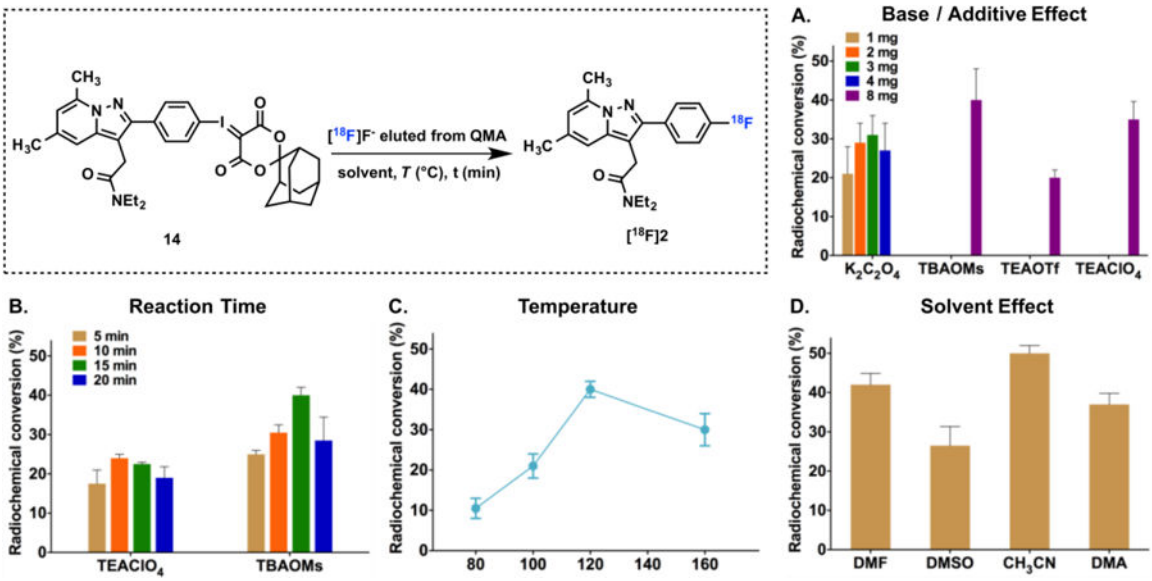

Figure 2.

Radiolabeling optimization for **[^{18}F]2**. [^{18}F]fluoride (37–111 MBq; 1–3 mCi) was used in each reaction. (A) Precursor (2 mg), DMF (0.4 mL), 120 °C, 5 min; (B) Precursor (2 mg), $TEAClO_4$ or TBAOMs (12 mg), DMF (1.0 mL), 120 °C; (C) Precursors (2 mg), TBAOMs (12 mg), DMF (1.0 mL), heated for 15 min; (D) Precursors (2 mg), TBAOMs (12 mg), solvent (1.0 mL), 120 °C, 15 min. Radiochemical conversion and product identity were assessed by radioTLC and radioHPLC, respectively.

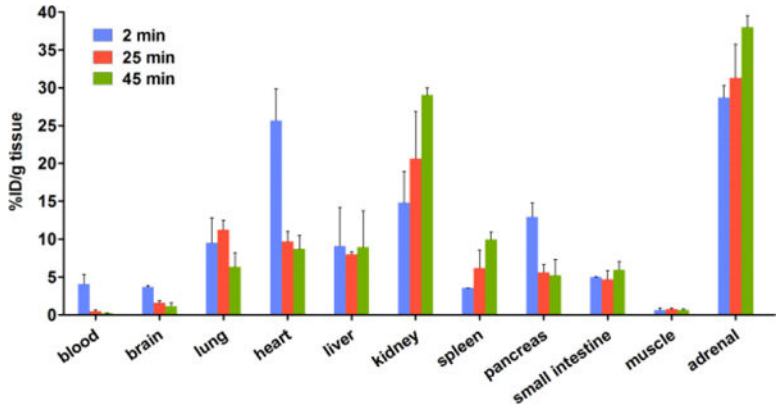

Figure 3.

Ex vivo biodistribution of **[^{18}F]2** in mice. Data are expressed as %ID/g (mean ± SD, n = 3).

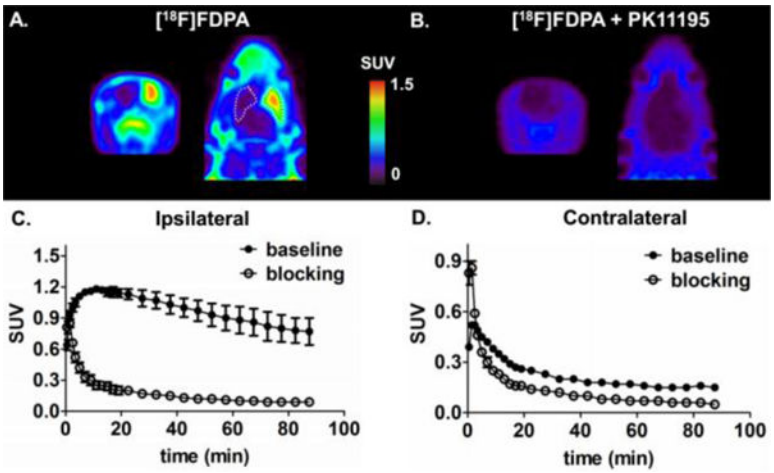

Figure 4.

PET images (summed 0–90 min) (A,B) and time activity curves (C,D) for baseline and blocking with PK11195.

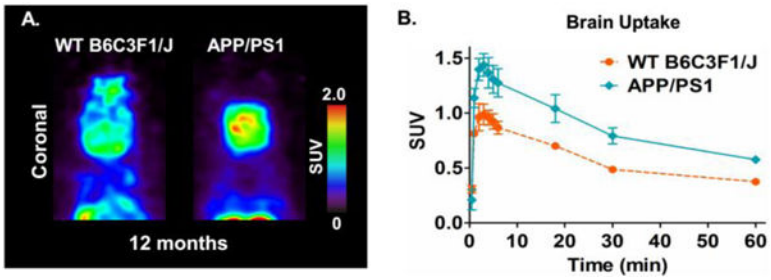

Figure 5.

PET Imaging studies in APP/PS1 mouse models for **[^{18}F]2** uptake. (A) Representative PET images (summed 0–30 min) between age-matched wild type and APP/PS1 mouse models; (B) time-activity curves (n = 2).

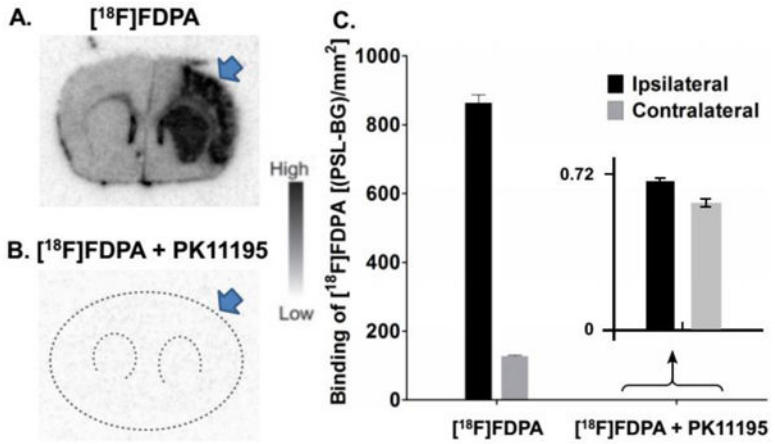

Figure 6.

In vitro autoradiography of **[^{18}F]2** in ischemic rat brains. Representative autoradiogram of **[^{18}F]2** alone (A) or with PK11195 (B). Arrows indicate ipsilateral side. Quantitative effects of PK11195 blocking (C).

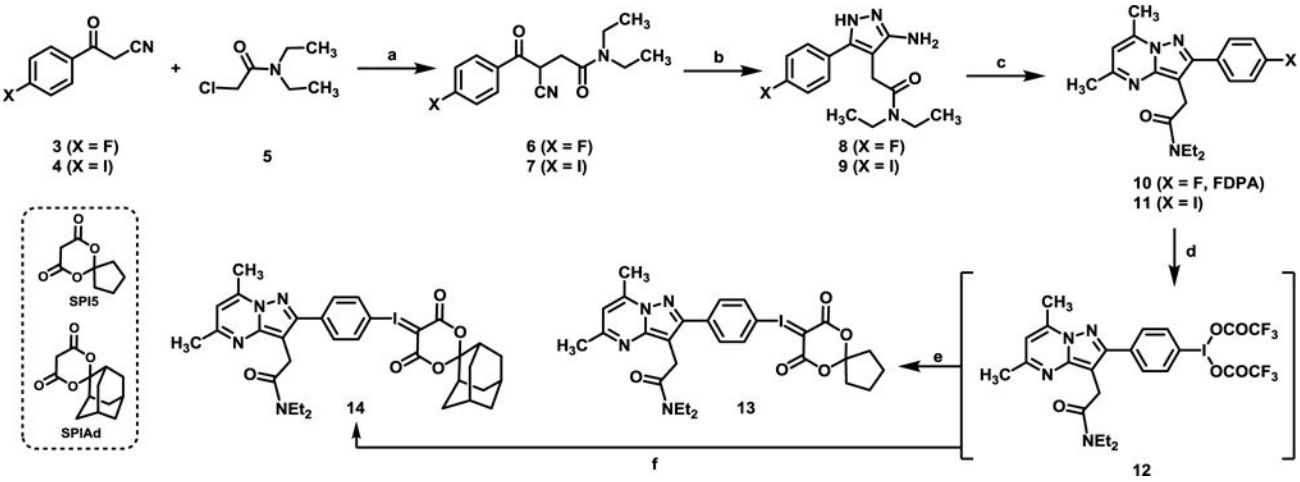

Scheme 1.

Syntheses of **10**, **11**, and SCIDY Precursors **13** and **14**[a]

[a]Reagents and conditions: (a) NaOH, NaI, microwave, 80 °C, 40 min, 80% EtOH in H_2O, 55% for **6**, 62% for **7**; (b) hydrazine, AcOH, 80 °C, 8 h, EtOH, 88% for **8**, 83% for **9**; (c) pentane-2,4-dione, 80 °C, 4 h, EtOH, 75% for **10**, 80% for **11**; (d) **11**, Oxone, TFA/$CHCl_3$ = 3/1, 23 °C, 1 h; (e) SPI5, 10% Na_2CO_3 (aq.), rt, 70 min, EtOH, 22% for **13** over two steps from **11**; (f) SPIAd, 10% Na_2CO_3 (aq.), rt, 70 min, EtOH, 34% for **14** over two steps from **11**.